Supporting Information

Correlating the Valence State of the Cu-Based Electrocatalyst for CO_2 Reduction to C_{2+}

Materials and Methods:

Chemicals:

Copper chloride (CuCl) and sodium oleate were purchased from Innochem. Potassium hydroxide (KOH) was purchased from Macklin. Hexamethylenetetramine ($C_6H_{12}N_4$), hydrazine hydrate ($N_2H_4 \cdot H_2O$), and ethanol (C_2H_5OH) were all purchased from Sinopharm. All chemicals were used as purchased without further purification. Ultrapure water (18.2 MΩ cm) was purified with an HHitech instrument.

Characterization:

The crystal phases of the samples were analyzed by X-ray diffraction (XRD, D/MAX-2550). The morphologies of the samples were determined by transmission electron microscopy (TEM, JEOL 200CX) and AC HAADF-STEM (JEOL JEM-ARM 200F). X-ray photoelectron spectroscopy (XPS) measurements were performed on a PHI5000 VersaProbe IV with monochromatic Al Kα radiation.

In situ attenuated total reflection surface-enhanced infrared absorption spectroscopy (ATR-SEIRAS):

In situ ATR-SEIRAS was carried out on a Bruker INVENIO-R FT-IR spectrometer equipped with a Pike Technologies VeeMAX III ATR accessory. The Au-coated Si semi-cylindrical prism (20 mm in diameter) was used as the conductive substrate for catalysts and the IR reflection element. The catalyst suspensions were dropped on the Au/Si surface as the working electrode. The mass loading of the catalyst was 1 mg/cm^2 and the electrolyte was 1 M KHCO$_3$. In situ ATR-SEIRAS spectra were recorded while the working electrode potential was stepping.

In situ Raman spectroscopy:

In situ Raman spectroscopy was carried out by using a Horiba LabRAM HR Evolution Raman microscope. The laser wavelength was controlled at 633 nm. 1 M KOH aqueous solution was used as an electrolyte. The gas diffusion layer (29 BC) coated with catalyst Ag/AgCl electrode, and carbon rod were used as working electrode, reference electrode, and counter electrode, respectively.

CO_2 Electrochemical measurements:

The experiments were performed in a three-compartment microfluidic flow cell (Gaoss Union (Tianjin) Photoelectric Technology Company, Tianjin, China) separated by a fuma membrane. And a carbon paper (2×0.5 cm^2) as the cathode. The Ag/AgCl reference electrode was located inside the cathode compartment. A total of 10 mg catalyst and 50 μL of 5 wt% Nafion solution were first dispersed in 500 μL of water and 500 μL of ethanol under the assistance of an ultrasonic processor for 10 min. After vacuum drying, a real 2×0.5 cm^2 gas diffusion electrode was assembled into a flow cell electrolyzer as the working electrode. During the measurements, CO_2 gas was directly fed to the cathode GDL at a rate of 100 sccm (outlet flow speeds). The catholyte was 1 M KOH aqueous solution was used as the electrolyte both in the cathode and anode compartments. It was forced to continuously circulate through the cathode compartment at a rate of 5 mL/min. All the applied cathode potentials after iR_{cell} compensation (i is the applied current and R_{cell} is the cell resistance) were converted to the RHE reference scale using $E_{RHE} = E_{Ag/AgCl} + 0.197$ V $+ 0.0591 \times$ pH-i$\times R_{cell}$. The R_{cell} is determined by performing an electrochemical impedance spectroscopy measurement using a Chenhua 760e electrochemical workstation carried out from 100 kHz to 0.1 Hz with an amplitude of 5 mV at open-circuit voltage. For gaseous products, 100 mL of gas extracted from a gas bag was injected into gas chromatography (GC, GC9790II; FULI, China) with a thermal conductivity detector (TCD) detector using high purity N_2 as carrier gas. Quantification of the gaseous

products was performed with the conversion factor derived from the standard calibration gases. For liquid products, 500 μL of electrolyte, 200 μL of D_2O and 0.1 μL of DMSO solution were mixed and then detected by ^{1}H nuclear magnetic resonance (^{1}H NMR, AVANCE NEO 400; Bruker, Germany). Faradaic efficiency was calculated as follows:

For gaseous products,

$$FE(\%) = \frac{Q_{gas}}{Q_{total}} = \frac{\upsilon \times t \times \delta/V_m \times N \times F}{i_{total} \times t} = \frac{\upsilon \times \delta/V_m \times N \times F}{i_{total}} \times 100\%$$

F: Faradaic constant: 96500 C/mol.

V_m: the molar volume of gas: 24 L/mol.

N: the number of electrons transferred for production formation, $N_{CO} = 2$; $N_{H2} = 2$; $N_{C2H4} = 12$; $N_{CH4} = 8$.

υ: the flow rate of CO_2.

δ: the measured gas product concentration in the GC sample loop.

i_{total}: the total current.

Q: charge number.

For liquid products,

$$FE(\%) = \frac{Q_{liquid}}{Q_{total}} = \frac{n_{liquid} \times N \times F}{Q_{total}} = \frac{n_{DMSO} \times S_{liquid}/S_{DMSO} \times N \times F}{Q_{total}} \times 100\%$$

n_{DMSO}: internal standard DMSO mole.

S_{liquid}: HCOOH, CH_3COOH, CH_3CH_2OH, and $CH_3CH_2CH_2OH$ peak area in NMR spectra.

N: the number of electrons transferred for production formation, $N_{HCOOH} = 2$, $N_{CH3COOH} = 8$, $N_{CH3CH2OH} = 12$, $N_{CH3CH2CH2OH} = 18$.

S_{DMSO}: DMSO peak area in NMR spectra.

Experimental Section:

Synthesis of Cu@Cu$_2$O NPs:

The Cu@Cu$_2$O-oleate complex intermediate was synthesized by a hydrothermal method. In a typical procedure, 99 mg CuCl, 914 mg sodium oleate (NaOA), 831 mg hexamethylenetetramine (HMT), and 100 µL N$_2$H$_4$·H$_2$O were added into 40 mL distilled water orderly. After vigorous stirring for 10 min, the mixed solution was transferred into a 100 mL Teflon cup and heated in a sealed autoclave at 100 °C for 24 h. Upon cooling to room temperature naturally, the final product was collected by centrifuging the mixture, washed with distilled water and absolute ethanol twice, and then dried in vacuum at 60 °C overnight for further analysis.

Preparation of CuO NPs:

Once the Cu@Cu$_2$O-oleate complex intermediate is fully dried, it is placed evenly in a porcelain boat and tightly sealed with tin foil. The porcelain boat was heated in a tube furnace to 300 °C (at 5 °C/min) in an airflow for 1h to yield CuO particles. The CuO particles were directly used without any treatment.
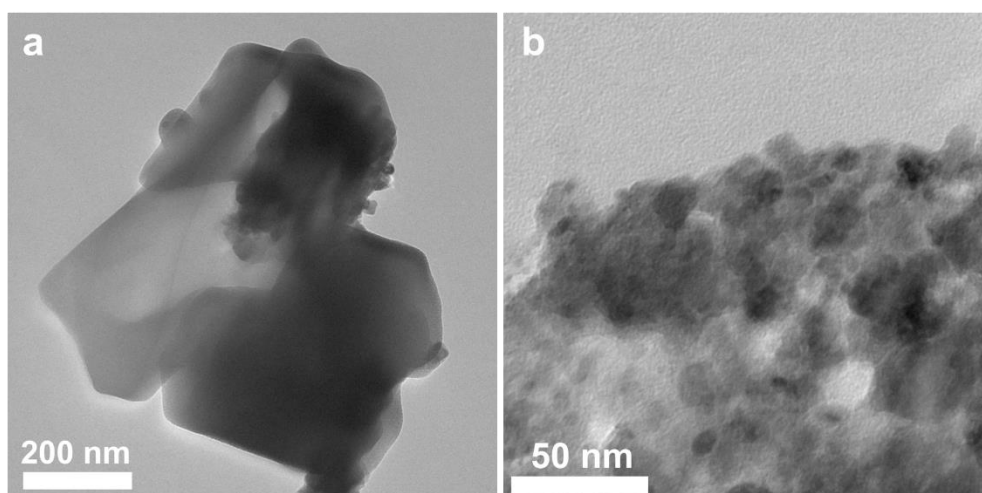
Supporting Figures:

Fig. S1: The TEM images of (a) CuO and (b) Cu@Cu$_2$O after CO$_2$RR electrocatalysis.
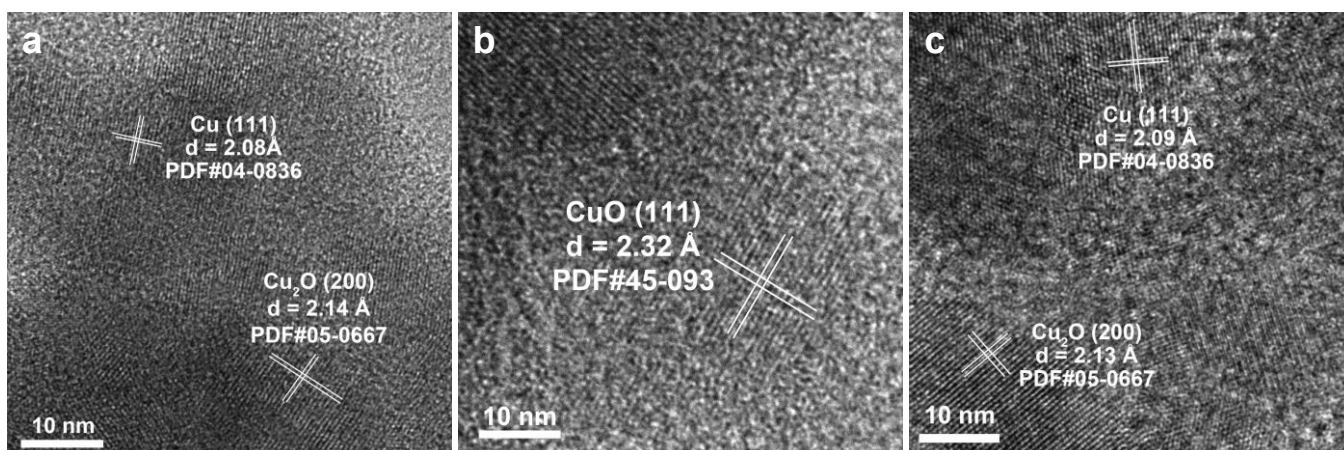

Fig. S2: The HRTEM images of (a and b) CuO and (c) Cu@Cu$_2$O after CO$_2$RR electrocatalysis.
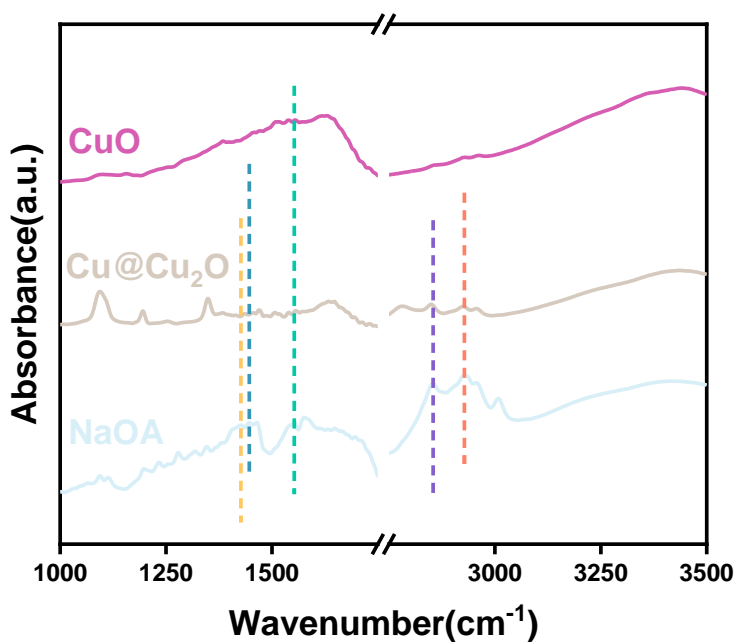
Fig. S3: FT-IR spectra of CuO, Cu@Cu$_2$O and NaOA. The two absorption peaks located at 2851 cm^{-1} and 2921 cm^{-1} can be ascribed to the C-H single bonds inherent in the methyl (-CH$_3$) and methylene (-CH$_2$-), respectively. The peak at 1560 cm^{-1} aligns with the asymmetric stretching vibration of the -COO-. Concurrently, the absorption peaks, positioned at 1446 cm^{-1} and 1425 cm^{-1}, are indicative of the symmetric stretching vibrations of the -COO-.
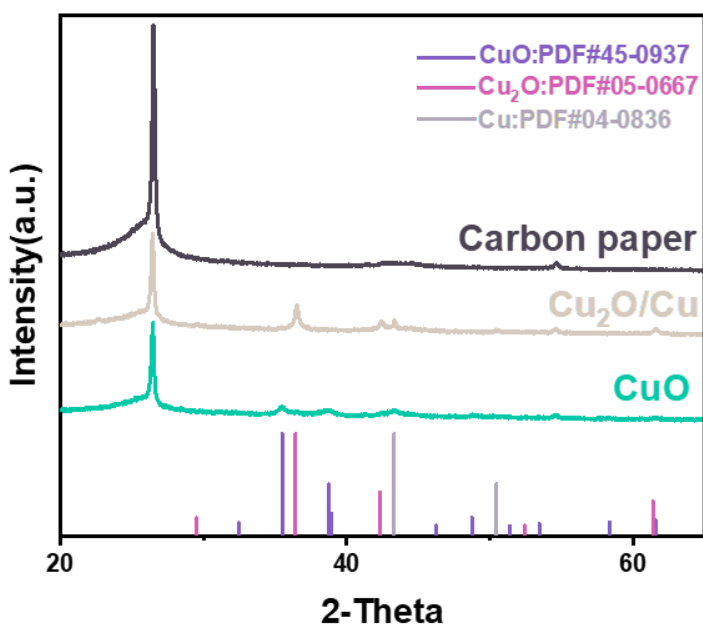
Fig. S4: The XRD patterns of CuO and Cu@Cu$_2$O supported on the carbon paper after CO$_2$RR electrocatalysis.
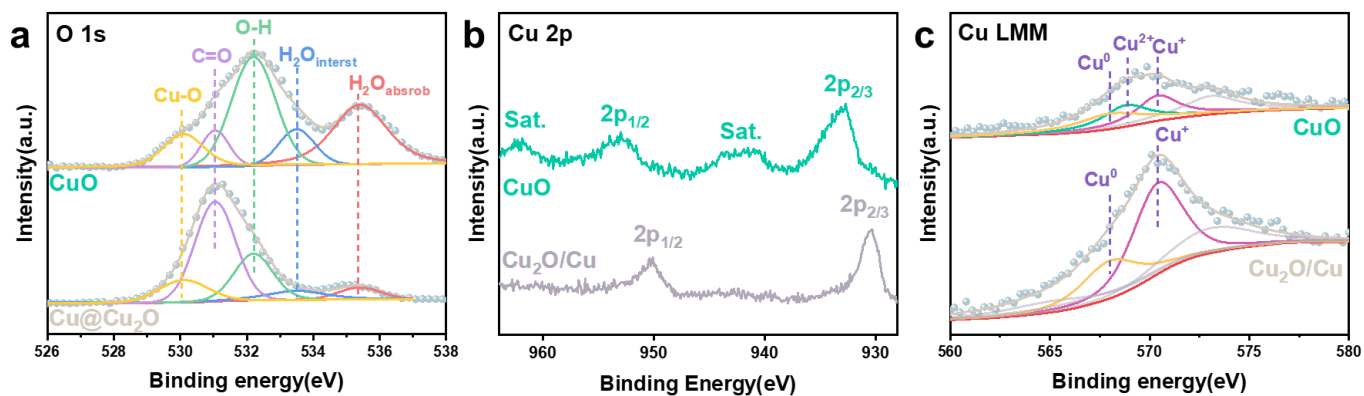
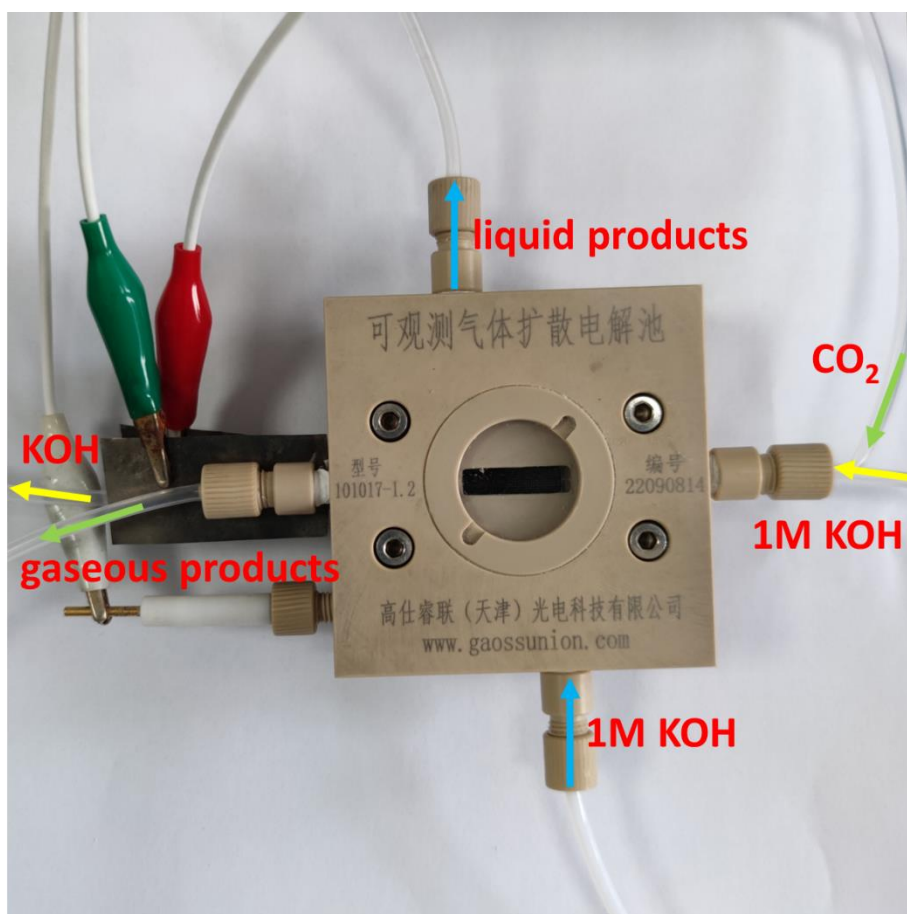**Fig. S5:** The XPS spectra of (a) O1s, (b) Cu2p, and (c) Cu LMM Auger spectra of the CuO and Cu@Cu$_2$O.

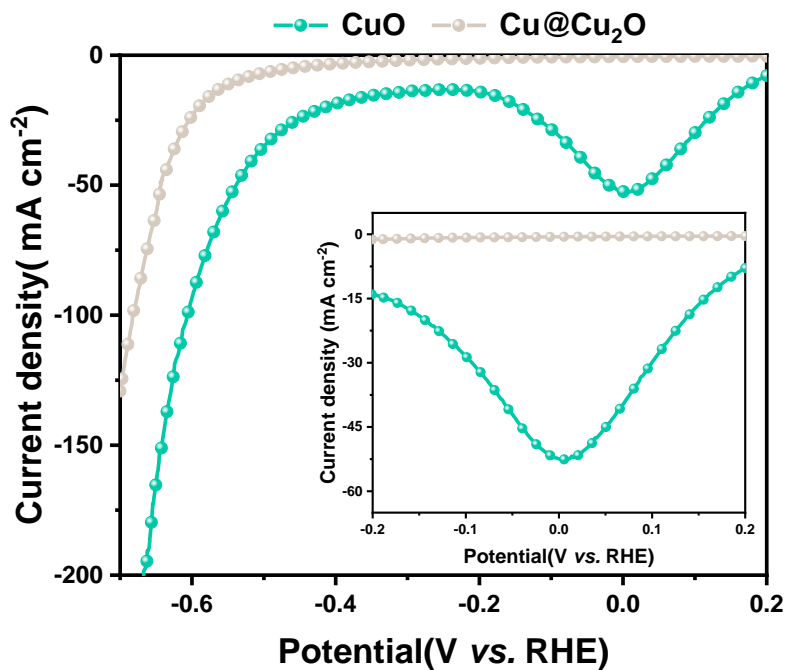**Fig. S6:** The photograph of the three-compartment microfluidic flow cell.

Fig. S7: Polarization curves of CuO and Cu@Cu$_2$O for CO$_2$RR at a scan rate of 50 mV/s.
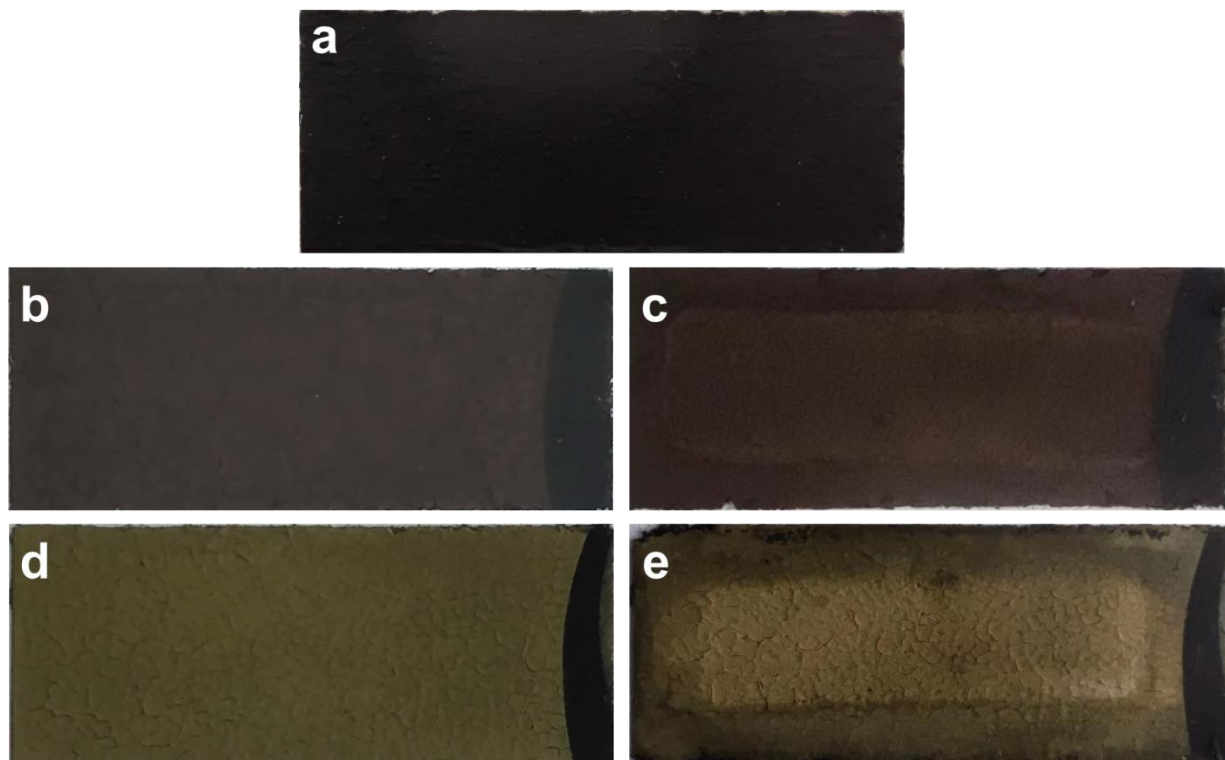

Fig. S8: The color of (a) carbon paper, color changes of (b and c) CuO, and (d and e) Cu@Cu$_2$O supported on the carbon paper after CO$_2$RR electrocatalysis.
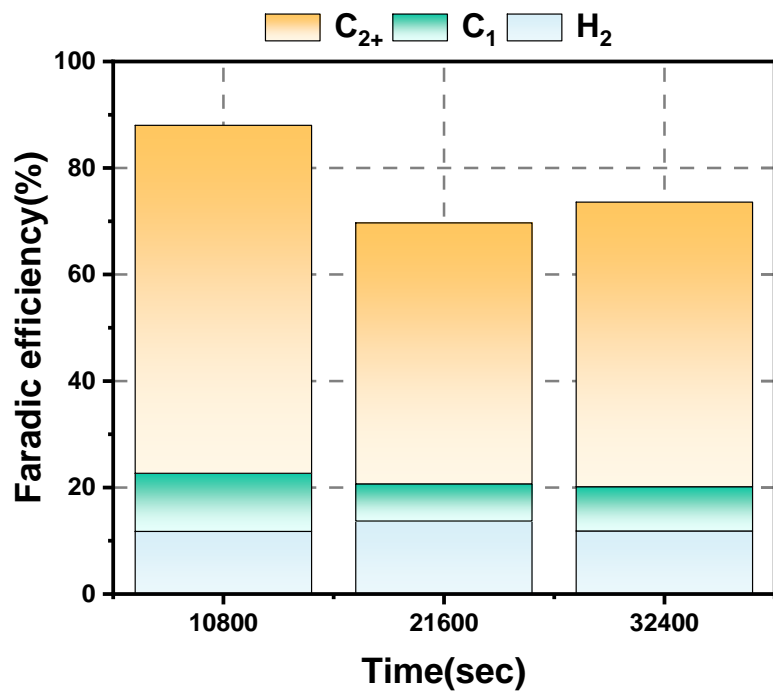
Fig. S9: Stability test of CuO electrolysis at 3, 6, and 9 hours.